Rate of ATP Synthesis by Dynein†

Erika L. F. Holzbaur and Kenneth A. Johnson*
Department of Molecular and Cell Biology, The Pennsylvania State University, University Park, Pennsylvania 16802
Received June 3, 1985

ABSTRACT: The rates of ATP synthesis and release by the dynein ATPase were determined in order to estimate thermodynamic parameters according to the pathway:

$$E + ATP \underset{k_{-1}}{\overset{k_1}{\rightleftharpoons}} E\text{-}ATP \underset{k_{-2}}{\overset{k_2}{\rightleftharpoons}} E\text{-}ADP\text{-}P_i \underset{k_{-3}}{\overset{k_3}{\rightleftharpoons}} E\text{-}ADP + P_i \underset{k_{-4}}{\overset{k_4}{\rightleftharpoons}} E + ADP + P_i$$

Dynein was incubated with high concentrations of ADP and P_i to drive the net synthesis of ATP, and the rate of ATP production was monitored fluorometrically by production of NADPH through a coupled assay using hexokinase and glucose-6-phosphate dehydrogenase. The turnover number for the rate of release of ATP from 22S dynein was 0.01 s^{-1} per site at pH 7.0, 28 °C, assuming a molecular weight of 750 000 per site. The same method gave a rate of ATP synthesis by myosin subfragment 1 of 3.4×10^{-4} s^{-1} at pH 7.0, 28 °C. The rate of ATP synthesis at the active site was estimated from the time dependence of medium phosphate–water oxygen exchange. Dynein was incubated with ADP and [^{18}O]P_i, and the rate of loss of the labeled oxygen to water was monitored by ^{31}P NMR. A partition coefficient of 0.31 was determined, which is equal to $k_{-2}/(k_{-2} + k_3)$. Assuming $k_3 = 8$ s^{-1} [Johnson, K. A. (1983) *J. Biol. Chem. 258*, 13825–13832], $k_{-2} = 3.5$ s^{-1}. From the rates of ATP binding and hydrolysis measured previously (Johnson, 1983), the equilibrium constants for ATP binding and hydrolysis could be calculated: $K_1 = 5 \times 10^7$ M^{-1} and $K_2 = 14$. Thus, ATP binding, not hydrolysis, is accompanied by a large free-energy change, and this binding energy is used to establish the pathway both kinetically and thermodynamically by driving the rapid dissociation of dynein from the microtubule.

The two major eukaryotic motility systems, actomyosin and microtubule–dynein, both use the energy of ATP hydrolysis to drive the sliding of adjacent filaments to produce macroscopic movement [for a review, see Johnson (1985)]. Dynein isolated from *Tetrahymena* cilia is a three-headed ATPase with a molecular weight of 1.9×10^6. The three globular heads are attached to the A tubule of the outer doublet by three apparently flexible strands and interact transiently with the adjacent B subfiber in a reaction coupled to movement. Previous studies have shown that all three globular heads associate with the microtubule in the absence of ATP and the binding of ATP to each head induces a rapid dissociation of dynein from the microtubule (Porter & Johnson, 1983a,b). Hydrolysis of the ATP occurs more slowly on the free dynein molecule (Johnson, 1983), which may then rebind to the microtubule before the release of products as shown in the preceding paper (Omoto & Johnson, 1986).

In the absence of microtubules, the kinetics of the dynein ATPase pathway can be modeled as shown in Scheme I, where k_1, the rate of ATP binding, was determined by stopped-flow and chemical-quench-flow methods to be 4.7×10^6 M^{-1} s^{-1} (Porter & Johnson, 1983b; Johnson, 1983). In addition, rapid chemical-quench-flow studies have provided a measurement of the rate of ATP hydrolysis on the enzyme, $k_2 + k_{-2} = 60$ s^{-1}. Product release is rate limiting in the steady state, $k_3 = 2$–8 s^{-1}.

Scheme I

$$E + ATP \underset{k_{-1}}{\overset{k_1}{\rightleftharpoons}} E\text{-}ATP \underset{k_{-2}}{\overset{k_2}{\rightleftharpoons}} E\text{-}ADP\text{-}P_i \underset{k_{-3}}{\overset{k_3}{\rightleftharpoons}} E\text{-}ADP + P_i \underset{k_{-4}}{\overset{k_4}{\rightleftharpoons}} E + ADP + P_i$$

Kinetic studies have established the pathway of the cross-bridge cycle, but the thermodynamics of the pathway must be assessed in order to understand the mechanism by which the chemical energy from ATP hydrolysis is coupled to produce mechanical energy for motility. The pathway of the ATPase is determined kinetically by the binding of ATP which induces a rapid dissociation of the microtubule–dynein complex (Porter & Johnson, 1983; Johnson, 1983, 1985). This implies that the major free-energy changes in the dynein ATPase pathway may occur with nucleotide binding and that it is the tight binding of the nucleotide to the enzyme which drives the dissociation of dynein from the microtubule. To test this hypothesis, k_{-1}, the rate of release of ATP from dynein, and k_{-2}, the rate of ATP synthesis on the enzyme, were measured. The equilibrium constants for these two steps were then calculated from the rates of the forward and reverse reactions.

Medium phosphate–water oxygen exchange studies were performed in order to determine the rate of synthesis of ATP by dynein. These studies established a minimum estimate for the rate of ATP synthesis at the active site. Combined with measurements of the net rate of production of free ATP, these studies indicate that ATP release is rate limiting under conditions of net synthesis from ADP and phosphate. Thus, the rate of ATP release could be measured as the rate of production of free ATP upon incubation of dynein with high concentrations of ADP and phosphate with a fluorescence coupled assay system of hexokinase and glucose-6-phosphate dehydrogenase. This system provides both a sensitive measure of ATP production in real time and a method of entrapping the ATP released by the dynein before it can rebound and be hydrolyzed by the ATPase.

Experimental Procedures

Preparation of Proteins. Dynein was prepared according to the method of Porter & Johnson (1983a). For the experiments measuring the net rate of ATP production, the dynein

†Supported by National Institutes of Health Grant GM26726. K.A.J. was supported by an Established Investigatorship of the American Heart Association with funds contributed in part by the Pennsylvania Affiliate.
*Correspondence should be addressed to this author.

0006-2960/86/0425-0428$01.50/0

could not be purified on sucrose gradients because even low levels of sucrose were found to be inhibitory to the coupled assay. Thus, the dynein was purified instead by layering onto 12-mL gradients of 7–40% glycerol in 50 mM piperazine-*N*,*N*′-bis(2-ethanesulfonic acid) (PIPES)[1] and 4 mM $MgCl_2$ and centrifuging for 13.5 h at 32000 rpm (175000*g*) or for 11.3 h at 35000 rpm (209000*g*) using an SW 41 Ti rotor. Analysis of the fractions by gel electrophoresis and ATPase measurements (data not shown) confirmed that the protein was not detectably different than that reported previously using sucrose gradients (Porter & Johnson, 1983a). The pooled 22S dynein fractions were dialyzed vs. 50 mM PIPES and 10 mM $MgCl_2$ for 2–3 h. The dialysis tubing was packed in poly(ethylene glycol) on ice for 1 h to concentrate the dynein to about 2 mg/mL and then dialyzed overnight.

Dynein concentrations were determined by the absorbance at 280 nm using an extinction coefficient of 0.97 cm^2/mg (D. B. Clutter, D. Stimpson, V. A. Bloomfield, and K. A. Johnson, unpublished results), and by assuming a molecular weight of 750000 per site (Johnson, 1983; Shimizu & Johnson, 1983b).

Myosin was isolated from rabbit back and leg muscles (Weeds & Taylor, 1975). Myosin subfragment 1 (S-1) was produced by digestion with 0.05 mg/mL α-chymotrypsin. The reaction was stopped after 20 min by the addition of 0.1 mM phenylmethanesulfonyl fluoride. The myosin S-1 was purified by DEAE-Sephacel column chromatography with a gradient of 25–200 mM KCl in 50 mM imidazole. The A1 and A2 peaks were pooled and concentrated by ammonium sulfate fractionation. The concentration of chymotryptic S-1 myosin was determined by the absorbance at 280 nm using an extinction coefficient of 0.75 cm^2/mg (Weeds & Pope, 1976).

Purification of ADP. ADP (Sigma grade III) was purified to remove contaminating nucleotides by chromatography on DEAE-Sephadex A25 with an elution gradient of 0.2–0.5 M NH_4HCO_3. The purity of the ADP was verified by thin-layer chromatography on PEI–cellulose developed with 0.85 M KH_2PO_4. The concentrations of ADP and ATP were determined by the absorbance at 260 nm using an extinction coefficient of 15.0 cm^2/μmol for adenine at pH 7.0.

Assay for ATP Synthesis. To measure the rate of ATP synthesis by dynein, a coupled assay system of hexokinase and glucose-6-phosphate dehydrogenase (Bergmeyer, 1963; Lowry & Passonneau, 1972) was employed. The formation of NADPH was monitored by following the increase in fluorescence which is directly related to the production of ATP within the assay system. A Perkin-Elmer MPF-44B fluorescence spectrophotometer was used for these experiments with excitation at 340 nm (5-nm slit) and emission measured at 455 nm (5-nm slit).

The assay system was composed of 150 units of hexokinase, 1 unit of glucose-6-phosphate dehydrogenase (the assay enzymes were the lyophilized form from yeast, from Boehringer Mannheim), 0.39 mM $NADP^+$, 2 mM ADP, 4 mM glucose, 4 mM phosphate, 1 μM diadenosine pentaphosphate (Ap_5A) (Lienhard & Secemski, 1973; Feldhaus et al., 1975; Goody et al., 1977), and 10 mM $MgCl_2$ in 50 mM PIPES. These components were contained in a total volume of 0.5 mL in a cuvette with a 5-mm path length thermostated to 28 °C.

The observed fluorescence signal was standardized to known ATP concentrations for each set of experiments. A small volume of ATP solution of known concentration was added to the cuvette, and the amplitude of the change in fluorescence was recorded. The precision of the resulting standard curves was high and demonstrated the sensitivity and reliability of this technique for the detection of micromolar concentrations of ATP.

For each rate measurement, the individual assay components were mixed at 4 °C, dynein or myosin was then added, the cuvette was transferred to the 28 °C constant-temperature holder, and the increase in fluorescence with time was monitored. Mixing the assay components at 0 °C immediately prior to running a time course and then quickly warming the system to 28 °C were found to give the lowest blank rate. As illustrated in Figure 4, and initial change in fluorescence due to the warming of the assay system to 28 °C was followed by a linear increase which continued for longer than 30 min.

For each set of experiments, the blank rate of the assay system was determined and corrected for. Because it was necessary to use high concentrations of components of the assay system to maximize the efficiency of the trapping reaction, the blank rate was not always equal to zero.

ATPase Activity Assays. ATP hydrolysis rates were measured at 25 °C, pH 7.0. Excess ATP (1 mM) was added to a solution 100 μg/mL in dynein at time zero. An aliquot was withdrawn for each time point and mixed with an equal volume of 2 N perchloric acid. The resulting inorganic phosphate concentrations were determined by the malachite green phosphate assay (Lanzetta et al., 1979).

Chemical Quench Flow. Quench-flow experiments were performed as described (Johnson, 1983). The temperature was regulated was regulated to 28 °C. Dynein was first mixed either with ADP and P_i in 50 mM PIPES and 10 mM $MgCl_2$, pH 7, buffer or with the buffer only and then mixed in the quench-flow apparatus with ATP and [^{32}P]ATP to yield final concentrations of 0.2 mg/mL dynein and 0.025 μM ATP with or without 2 mM ADP and 4 mM P_i. Rapid-quench time points between 10 ms and 10 s were obtained by using a quench-flow apparatus designed and constructed in this laboratory. This apparatus will be described in more detail at a later date (K. A. Johnson, unpublished results). Briefly, 20-μL samples were loaded into segments of tubing using three-way Hamilton valves. The position of the three-way valve was then changed to allow drive syringes containing buffer to force the reactants through a T mixer, then through a variable-length segment of tubing, and then into a quench solution. The length of tubing leader to the quench solution was varied to obtained time points from 10 to 100 ms. The syringes containing buffer were driven by using a ball screw and a stepping motor as described by Froelich et al., (1976). The programmable stepping motor provided precisely controlled movements of the drive syringes including essentially instantaneous start/stop at full speed (1000 steps per second). Reaction times longer than 100 ms were obtained by driving the syringes once to force the mixing of reactants, pausing for a defined interval of time, and then driving the syringes a second time to quench the reaction.

Medium Phosphate–Water Oxygen Exchange Studies. Highly enriched [^{18}O]P_i was prepared by reacting PCl_5 with 99% $H_2{}^{18}O$ obtained from Miles Laboratories (Risley & Van Etten, 1978). The resulting phosphate was purified by ion-exchange chromatography on a Bio-Rad AG1-X8 (Cl^- form) column. An enrichment of 97% ^{18}O was achieved. Medium exchange reactions were conducted at 28 °C in 50 mM PIPES, 4 mM $MgCl_2$, 1 mM EGTA, and 5 μM diadenosine pentaphosphate at pH 7. Aliquots of 1 mL were removed from the reaction mixture at various times and mixed vigorously with

[1] Abbreviations: EGTA, ethylene glycol bis(β-aminoethyl ether)-*N*,*N*,*N*′,*N*′-tetraacetic acid; PIPES, piperazine-*N*,*N*′-bis(2-ethanesulfonic acid); EDTA, ethylenediaminetetraacetic acid; S-1, subfragment 1; PEI, poly(ethylenimine).

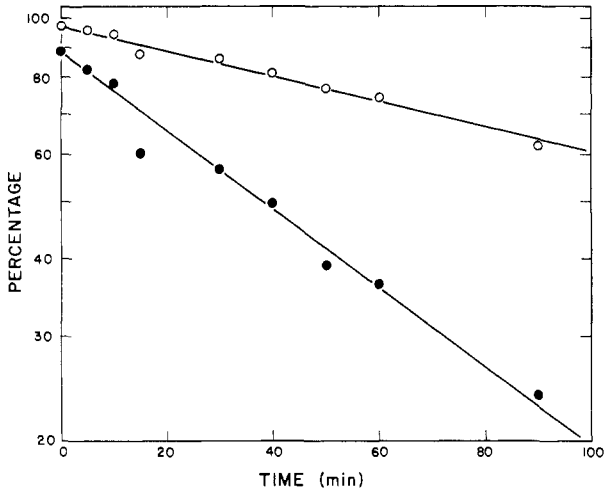

FIGURE 1: Time course of medium exchange. The reaction mixture contained 0.1 μM 22S dynein, 100 μM ADP, 20 mM [^{18}O]P_i, and 5 μM adenosine pentaphosphate in 50 mM PIPES, 4 mM $MgCl_2$, and 1 mM EGTA, pH 7. The two curves show the loss of the fully labeled [$^{18}O_4$]P_i species (●) and the average ^{18}O enrichment from the phosphate with time (○).

chloroform to stop the reaction. After extraction, the aqueous phases were lyophilized and resuspended in 1.5 mL of 50 mM EDTA in D_2O. EDTA chelates any metal ions present and prevents peak broadening during ^{31}P NMR analysis. The pH of the resulting solutions was adjusted to 9–10 by addition of base. All glassware was washed with 1 N HNO_3 to prevent contamination by residual phosphate.

The samples in 50% D_2O were analyzed on a Bruker 360-MHz superconducting NMR spectrometer. To resolve the peaks of the phosphate species, ^{31}P NMR spectra were measured at a frequency of 145.805 Hz (Cohn & Hu, 1978). A total of 225 scans were averaged for each of the spectra. The $P^{18}O_4$, $P^{18}O_3{}^{16}O_1$, $P^{18}O_2{}^{16}O_2$, $P^{18}O_1{}^{16}O_3$, and $P^{16}O_4$ peaks were each separated by shifts of 0.02 ppm. The observed [^{18}O]P_i distributions were compared to calculated best fits based on the partition coefficient by using a computer program modified from the work of Hackney (1980).

RESULTS

Medium Phosphate–Water Oxygen Exchange. The time course of medium exchange was determined by reacting 0.1 μM dynein with 100 μM ADP and 20 mM [^{18}O]P_i at 28 °C, pH 7. Aliquots were removed from the reaction solution at intervals and treated as described under Experimental Procedures. A logarithmic plot of the time dependence of the wash out of ^{18}O is shown in Figure 1. The partition coefficient (P_c) for the exchange reaction can be calculated according to the equation $P_c = (4 - R_4)/3$ where R_4 is the rate of loss of [$^{18}O_4$]P_i divided by the rate of loss of the average ^{18}O enrichment of the phosphate (Hackney et al., 1980). From the time course illustrated, the partition coefficient was determined to be 0.322. The average value was $P_c = 0.31 \pm 0.01$ ($n = 4$).

The exchange reaction was examined in the absence of ADP or in the presence of vanadate. Reactions were run with 0.1 μM dynein in the absence of ADP or in the presence of 100 μM ADP and 200 μM vanadate for 2.5 h at 28 °C. In each case, NMR analysis of the resulting solution showed no discernible exchange; only the [$^{18}O_4$]P_2 peak was observed. Vanadate is a highly potent inhibitory of dynein (Shimizu, 1981) and binds to the active site in the presence of ADP to form an ADP–vanadate complex which may mimic the transition state for ATP hydrolysis (Shimizu & Johnson, 1983a).

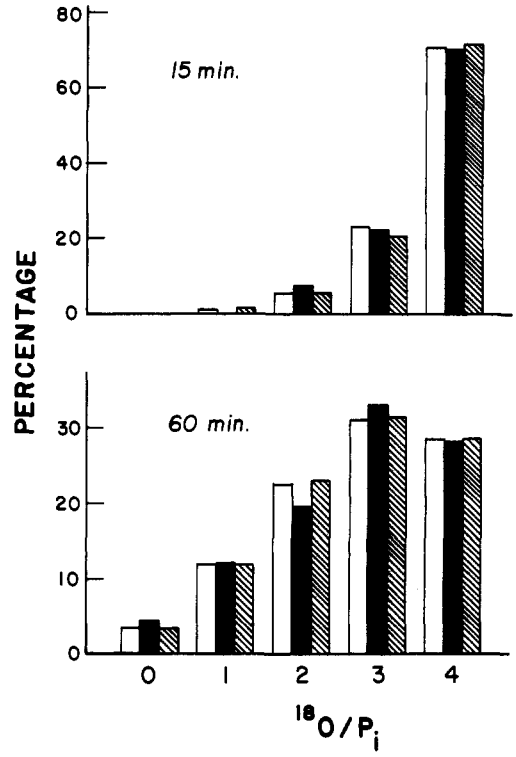

FIGURE 2: Comparison of the observed and theoretical [^{18}O]phosphate distributions. The observed distribution of [^{18}O]phosphate species (black bars) is compared at two times of incubation to the theoretical distributions calculated from a partition coefficient of 0.31 (hatched bars) or from the best fit to the data (white bars). The least-squares fit gave values of 0.23 and 0.33 at 15 and 60 min, respectively. The reaction conditions are as in Figure 1, but with 10 mM phosphate.

The lack of exchange in the absence of ADP or in the presence of vanadate indicates that the measured exchange of unlabeled water oxygens into the phosphate is most likely due to the catalytic activity of dynein in the synthesis and hydrolysis of ATP.

The exchange reaction was also examined at a lower concentration of phosphate (data not shown). The partition coefficient at 10 mM phosphate, 0.305, was the same within error as that measured at 20 mM phosphate. The absolute rate of exchange, as measured by the rate of loss of the fully labeled phosphate species, was 2.5×10^{-4} s^{-1} at 10 mM phosphate and 2.4×10^{-4} s^{-1} at 20 mM phosphate, the same rate within error. An approximate estimate of the rate of phosphate binding to the dynein–ADP complex can be obtained by dividing the observed rate of [$^{18}O_4$]phosphate loss by the partition coefficient and the concentration of dynein. This calculation gives a rate of 8000 M^{-1} s^{-1} per dynein site (0.1 μM site during the experiment). One should note that the observation that the rate was independent of phosphate concentration implies that the rate of phosphate binding did not reach saturation at the concentrations of phosphate used and thus the apparent second-order rate constant represents a single step kinetically. In addition, the rate constant must be considered as a minimum estimate because it is possible that not all of the enzyme sites were saturated by ADP. Further studies on the dependence of the rate of medium exchange on the concentrations of ADP and phosphate are currently under way in our laboratory.

With the use of a program based on transition probability functions (Hackney, 1980), the [^{18}O]phosphate isotopic distribution at each time point was calculated from the partition coefficient of 0.31. In Figure 2, the observed distributions at three times of incubation are compared to the theoretical

distributions expected for $P_c = 0.31$ and for the best fit to the data. The data are consistent with a single population of ATPases catalyzing exchange of the phosphate oxygens by a single mechanistic pathway. If there are differences between the three ATPase sites of dynein, they are not large enough to be detected by this method.

Net Synthesis of ATP. The rate of release of ATP from the dynein was measured by using a coupled enzymatic assay system to trap the ATP and to give a signal that could be monitored in renal time. We chose a system consisting of hexokinase and glucose to trap the ATP, and glucose-6-phosphate dehydrogenase to produce NADPH which could be detected fluorometrically with high sensitivity. The validity of this system was primarily dependent upon the ability of hexokinase to trap the ATP before it could rebind to the dynein. Therefore, to estimate the efficiency of the assay system, the rates of ATP entrapment by hexokinase and ATP hydrolysis by dynein were determined in separate experiments.

The rate of ATP utilization by hexokinase was measured in the fluorescence assay system by reducing the hexokinase concentration until the rate of synthesis of glucose 6-phosphate became rate limiting in the coupled conversion of ATP to NADPH. Under these conditions, the increase in fluorescence with time after the addition of ATP to the system is a direct measure of the rate of the hexokinase reaction. The resulting time course of the increase in fluorescence is shown in Figure 3A and was fit to a single exponential with a rate of 0.067 s^{-1}. Under usual assay conditions, hexokinase was present at 100 times this limiting concentration, so the measured rate was extrapolated to a value of 6.7 s^{-1} for entrapment of ATP by hexokinase.

The rate of ATP binding (and hydrolysis) by dynein at the high concentrations of ADP and P_i employed was determined by chemical-quench-flow methods. Dynein (0.2 mg/mL = 0.27 μM sites) was preincubated either with ADP and P_i in buffer or with buffer only and then rapidly mixed with a low concentration of [γ-^{32}P]ATP (0.025 μM). Reaction time points ranged from 0.1 to 20 s. The resulting data showing percent ATP hydrolysis with time are shown in Figure 3B. The rate of ATP hydrolysis was 1.1 s^{-1} in the absence and 0.18 s^{-1} in the presence of 2 mM ADP and 4 mM phosphate, respectively, thus showing a 6-fold inhibition by the ADP and phosphate. Because the experiment was performed with dynein in large escess over ATP, the observed pseudo-first-order rate divided by the dynein concentration is equal to the second-order rate constant for binding. The rate determined for ATP binding in the absence of ADP and P_i was 4.1 × 10^6 M^{-1} s^{-1}, which is comparable to the published rate of 4.7 × 10^6 M^{-1} s^{-1} (Porter & Johnson, 1983b). For the inhibited reaction, the rate is 6.7 × 10^5 M^{-1} s^{-1}. This implies that only one-sixth of the dynein sites were free and the remaining sites were occupied by ADP and/or phosphate. Moreover, this inhibition of the dynein ATPase under the conditions of the coupled assay system allows the rate of ATP production by dynein to be measured with less interference due to the rebinding and hydrolysis of ATP by dynein.

The rate of ATP binding and hydrolysis by myosin subfragment 1 was also measured in the presence of ADP and P_i. The rate was slow enough to allow the experiment to be performed by manual mixing and quenching over a time scale of 0–15 min. The observed rate of hydrolysis of 0.025 μM ATP by 2.4 μM S-1 in the presence of 2 mM ADP and 4 mM P_i was 5.6 × 10^{-3} s^{-1} at 28 °C in 50 mM PIPES (data not shown). This corresponds to a second-order rate constant of 2.3 × 10^3 M^{-1} s^{-1}, which represents a 3000-fold inhibition of

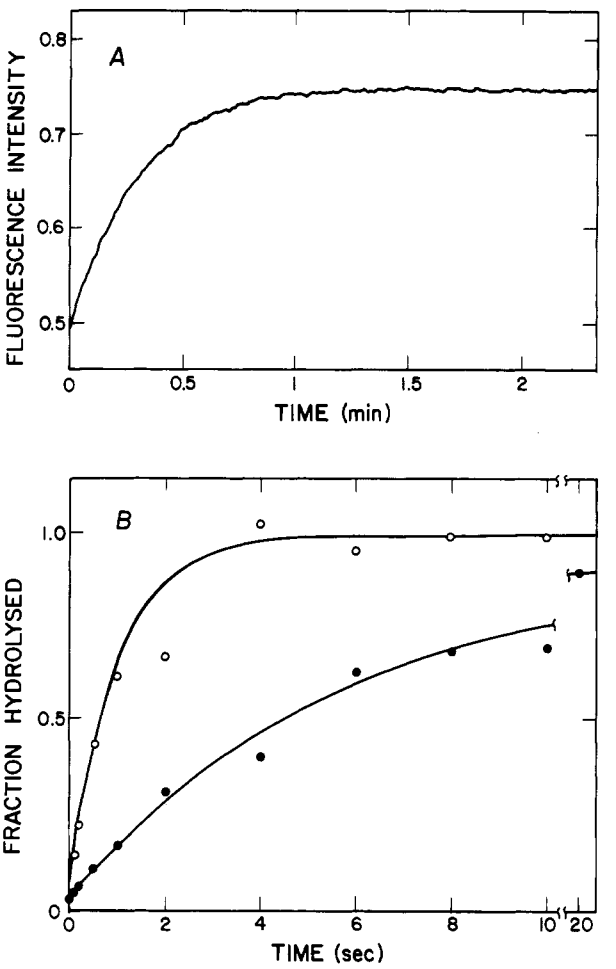

FIGURE 3: Rate of entrapment vs. rate of hydrolysis by dynein. (A) Rate of formation of glucose 6-phosphate from ATP and glucose with glucose in excess concentration. Hexokinase was present at 3 units/mL. ATP was added at an initial concentration of 7.7 μM. The other assay components were described under Experimental Procedures. Fluorescence intensity is described throughout the paper in arbitrary units that were calibrated to known concentrations of ATP. (B) Rate of dynein ATPase in the presence of high concentrations of ADP and phosphate. Reaction concentrations were 0.2 mg/mL 22S dynein and 0.025 μM ATP in the presence (●) or absence (○) of 2 M ADP and 4 mM phosphate.

the rate 6.6 × 10^6 M^{-1} s^{-1}, as determined by stopped-flow fluorescence measurements in the absence of ADP and P_i at 28 °C in 50 mM PIPES and 4 mM $MgCl_2$, pH 7.0 (T. J. Chilcote and K. A. Johnson, unpublished results). The marked inhibition of the ATPase allowed the rate of ATP synthesis by myosin S-1 to be measured efficiently over a wide range of concentrations by the assay system.

The application of the coupled assay to the measurement of the rate of ATP synthesis is illustrated in Figure 4A, which shows traces of increasing fluorescence with time upon incubation of various concentrations of dynein with the coupled assay system. The figure shows that the increase in fluorescence was linear and stable. The dynein concentration dependence is shown in Figure 5A for dynein concentrations ranging from 0 to 0.93 μM site (0.7 mg/mL). The illustrated data were measured in a single experiment with dynein from one preparation. The line follows a curve which is a function of the rate of ATP synthesis by dynein and the efficiency of the enzyme assay system, as described under Discussion. The fit to the line gives a turnover number of (9.7 ± 0.7) × 10^{-3} s^{-1} (Figure 5A).

Column-purified dynein has been shown to contain a low but measurable level of contaminating adenylate kinase activity

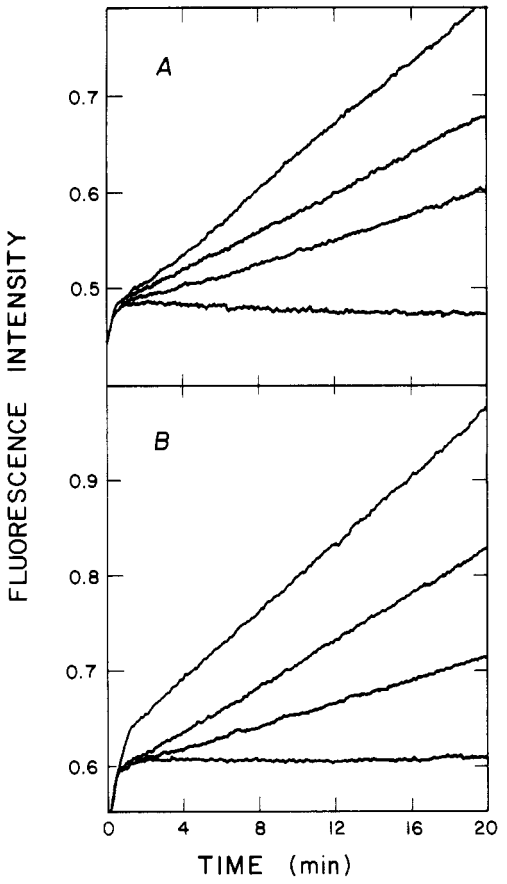

FIGURE 4: Time dependence of ATP synthesis for dynein and myosin. (A) Traces describing the rates of ATP synthesis by dynein at concentrations of 0, 0.21, 0.28, 0.55, and 0.82 μM dynein. Other assay system components were as described under Experimental Procedures. (B) Traces describing the rates of ATP synthesis by myosin at concentrations of 0, 4.6, 18.4, and 23.0 μM myosin subfragment 1. Assay conditions were as described under Experimental Procedures.

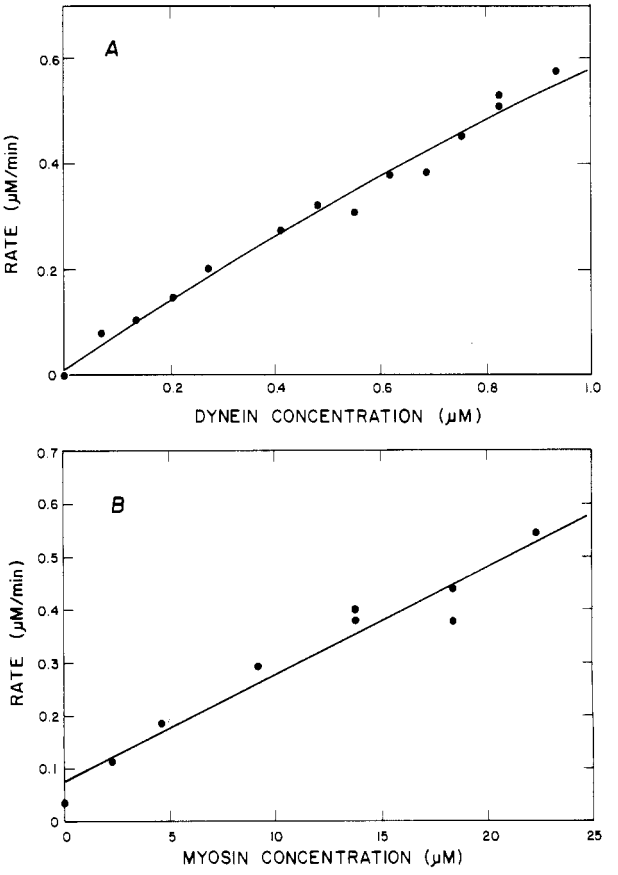

FIGURE 5: Concentration dependence of the rates of ATP synthesis by dynein and myosin. (A) Dependence of the rate of ATP synthesis on the concentration of dynein. The curve was drawn by determining the linear least-square fit to the corrected rates and then including the correction factor to calculate the curve. (B) Dependence of the rate of ATP synthesis on the concentration of myosin subfragment 1. The curve was fit as above. For both (A) and (B), the slopes of the curves describe the turnover number for the enzymes.

(Shimizu & Johnson, 1983a). Although the preparation of dynein used here was purified by an additional step, it was possible that the low rate of ATP production observed might be due to residual adenylate kinase contamination. To examine this possibility, the rate of ATP synthesis was determined in the presence and absence of 1 μM Ap_5A, a highly specific inhibitor of adenylate kinase (Lienhard & Secemski, 1973; Feldhaus et al., 1975). A 9% decrease in activity was found after the addition of Ap_5A. Most of this decrease was due to a decreased rate of the blank (without added dynein) after the addition of Ap_5A. With the inhibitor present in the assay system, a zero blank rate was observed, but without the inhibitor, this rate increased to approximately 0.05 μM ATP formed per minute. This indicates that the major source of contamination is from the enzymes of the coupled assay and not the gradient-purified dynein. To eliminate the contribution of adenylate kinase to the measured rate of ATP production, 1 μM Ap_5A was included in the assay system (Goody et al., 1977). Most importantly, the modest inhibition in rate upon the addition of Ap_5A demonstrates that the measured rate was not due to adenylate kinase. It was important to measure the rate in the absence as well as the presence of the inhibitor. If the rate was measured only in the presence of the inhibitor, one might have argued that the low rate was simply due to a contaminating adenylate kinase that was 99% inhibited.

The rate of synthesis of ATP by myosin subfragment 1 was also measured by using this assay system. Various concentrations of subfragment 1 were incubated with 2 mM ADP and 4 mM P_i. The increases in fluorescence with time are shown in Figure 4B, and the resulting concentration dependence of the rate is given in Figure 5B. A wider range of ATPase concentrations could be used with data up to 2.3 mg/mL (23 μM). The best fit to a line gives a turnover number of $(3.4 \pm 0.7) \times 10^{-4}$ s^{-1} at 28 °C, pH 7.0, in 50 mM PIPES.

Discussion

The experiments reported here provided estimates for the rates of synthesis and release of ATP by the dynein ATPAse. Combined with previous measurements for the rates of ATP binding and hydrolysis (Porter & Johnson, 1983b; Johnson, 1983), these data provide the first estimates for the free energy of ATP binding and hydrolysis by dynein. The important conclusion of these studies is that the major change in free energy occurs with ATP binding and not hydrolysis. These and previous studies point to the importance of nucleotide binding energy in establishing the kinetically and thermodynamically favored pathway for coupling energy transduction in the microtubule–dynein system.

The medium phosphate–water exchange was due to synthesis and hydrolysis of ATP at the active site of dynein. The measured partition coefficient, defining the probability that bound phosphate will react with ADP to synthesize ATP, is equal to $P_c = k_{-2}/(k_{-2} + k_3)$, according to Scheme I. For the present study, unhindered rotation of the enzyme-bound phosphate is assumed so that all P_i oxygens can participate in exchange (Hackney et al., 1980), but this remains to be established. Isotopic distributions calculated from a single

partition coefficient of 0.31 were compared to the data. Deviations from the calculated fit might suggest a nonhomogeneous ATPase population or an alternate exchange mechanism (Hackney et al., 1980). However, the calculated fits do closely model the observed distributions, as shown in Figure 2.

Preparations of glycerinated sea urchin sperm flagella and of sea urchin sperm flagellar dynein have previously been shown to catalyze medium and intermediate exchange reactions (Barclay & Yount, 1972; Kuleva et al., 1983). The medium exchange experiments described here extend these studies with a determination of the time course of the washout of label from [^{18}O]phosphate, monitored by ^{31}P NMR.

The rate of product release has been shown by chemical-quench-flow studies to be the rate-limiting step for steady-state turnover of ATP, with a rate of 8 s^{-1} (Johnson, 1983). In addition, vanadate inhibition studies have suggested that product release is ordered with phosphate followed by ADP (Shimizu & Johnson, 1983a). Therefore, if we assume that the rate-limiting step in the steady state is due to phosphate release, $k_3 = 8$ s^{-1}, then the rate of ATP synthesis, $k_2 = 3.5$ s^{-1}, can be calculated from the partition coefficient. The numbers quoted in this paper are based upon this assumption.

Alternatively, it is possible that phosphate release is faster than 8 s^{-1} and that the rate of ADP release is at least partially rate limiting. Preliminary experiments on the extent of medium exchange during net ATP hydrolysis suggest that this may be the case (E. L. F. Holzbaur and K. A. Johnson, unpublished results). If this is the case, our estimate of the rate of ATP synthesis (k_{-2}) will need to be increased, leading to a net decrease in the estimated free energy for ATP hydrolysis at the active site. However, this would only strengthen our conclusion that ATP hydrolysis occurs with a small change in free energy at the active site of dynein. Nonetheless, studies are currently under way to address this question.

The rate of ATP release was measured by using a coupled assay system. The efficiency of the assay system can be modeled in terms of two competing pathways for the ATP after its release into solution by dynein: entrapment by hexokinase at a rate k_h or rebinding and hydrolysis of dynein at a rate k_d. The disappearance of ATP follows the equation:

$$d[ATP]/dt = -(k_d[D] + k_h[H])[ATP]$$

where k_d and k_h are the second-order rate constants for the binding of ATP by dynein and the entrapment of ATP by hexokinase, respectively, and [D] and [H] are the concentrations of dynein and hexokinase, respectively. In this model, the fraction of released ATP that is measured by conversion to an NADPH fluorescence signal is $k_h[H]/(k_d[D] + k_h[H]$. The pseudo-first-order rate constant for ATP binding to hexokinase, $k_h[H]$, was determined to be 6.7 s^{-1} at the concentration of hexokinase used in the coupled fluorescence assay system. The apparent second-order rate constant for ATP binding by dynein in the presence of high concentrations of ADP and P_i (k_d) was measured by quench flow to be 6.7×10^5 M^{-1} s^{-1}.

Optimally, $k_h[H]$ would be much larger than $k_d[D]$, so that the efficiency of ATP entrapment would approach 100%. For the dynein concentrations examined (see Figure 5), the efficiencies of the system can be calculated from the fraction $k_h[H]/(k_d[D])$ and range from 99% down to 91% at the highest concentration of dynein used. In Figure 5A,B, the curves shown are the best fits calculated according to the variable efficiency of the system. For 22S dynein, the concentration dependence of the apparent rates describes a line with a best fit corresponding to a turnover number of 1.0×10^{-2} s^{-1}.

For myosin, the efficiency of entrapment is given by $k_h[H]/(k_m[M] + k_h[H])$ where $k_h[H] = 6.7$ s^{-1}, as above, [M] is the concentration of myosin subfragment 1, and k_m is the second-order rate constant for the binding of ATP to myosin in the presence of ADP and P_i, measured as 2.3×10^3 M^{-1} s^{-1}. At all myosin concentrations examined, the efficiency of entrapment exceeded 99%, so that the rate determination of 3.4×10^{-4} s^{-1} does not require correction.

Although the ATP binding rates of dynein and myosin are very similar in the absence of product inhibition, the two ATPases respond very differently to the presence of high concentrations of ADP and P_i. The rate for dynein is inhibited only 6-fold, but the rate for myosin is inhibited 3000-fold. This difference means that the rate of ATP synthesis can be measured in this system with a greater theoretical efficiency for myosin than for dynein. However, over the dynein concentration range examined in this study, the efficiency of measurement remained sufficiently high such that only a small correction was necessary.

To convert the measured turnover rate for the synthesis of ATP by dynein to an intrinsic rate constant for the release of ATP from the enzyme–ATP complex, the fraction of sites occupied by ATP must be considered. During the net synthesis of ATP in the presence of excess ADP and P_i, the release of ATP from the enzyme becomes rate limiting, and the step described by k_2 and k_{-2}, the synthesis and hydrolysis of ATP, approaches equilibrium. Thus, the measured turnover number is equal to the rate constant for release multiplied by the fraction of enzyme sites with ATP bound: $k_{obsd} = k_{-1}[E\text{–}ATP]/[E]_{total}$. The fraction of enzyme sites with ATP bound can be determined from the ratio k_{-2}/k_2, where k_{-2} is 3.5 s^{-1}, from the medium exchange experiments, and k_2 is 55 s^{-1}, as determined by chemical-quench-flow analyses (Johnson, 1983). The rate constant for ATP release is then equal to the measured turnover number divided by the fraction of sites with ATP bound, so that $k_{-1} = 0.1$ s^{-1}. In addition, if the concentrations of ADP and phosphate were not saturating, this measurement will be an underestimation of the true rate. We are currently determining the constants for ADP and for phosphate binding to dynein.

The equilibrium constant for ATP hydrolysis at the active site of myosin has been estimated to be approximately 4 (Taylor, 1977). This, combined with the present data, yields a rate constant for the release step of 2×10^{-3} s^{-1}. This rate is 5–10-fold greater than that measured previously (Cardon & Boyer, 1978). This difference may be explained in part by the differences in the temperature of measurement. These experiments were performed at 28 °C, whereas previous estimates were made at 21 °C.

Studies on myosin have also shown that the rate of release of ATP from myosin increases significantly in the presence of actin (Sleep & Hutton, 1978). Activation by tubulin of the rate of release of ATP from dynein could not be determined in this system. Further work is planned to address this question.

With the measured values for ATP binding and release, the free energy of ATP binding can be calculated. The reported value for the forward rate of ATP binding under the same conditions is 4.7×10^6 M^{-1} s^{-1} (Porter & Johnson, 1983b); with the value of 0.1 s^{-1} for the rate of ATP release, the binding constant for ATP is $\sim 5 \times 10^7$ M^{-1} ($K_d = 2 \times 10^{-8}$ M). Therefore, the binding of ATP to dynein is accompanied by a large negative change in free energy. In the cell, at a concentration of 1 mM ATP, the free-energy change for ATP binding would be $\Delta G = -13.6$ kJ/mol. In the cross-bridge

model of the dynein–microtubule cycle, ATP binding has been shown to induce the release of the dynein heads from the microtubules, and ATP hydrolysis then occurs on the free dynein molecule. Although the dynein–microtubule binding equilibrium has not yet been determined, it is clear that the large free-energy change accompanying ATP binding is sufficient to drive the dissociation of dynein from the microtubule and it is the substrate binding energy that is used to couple the free energy of ATP hydrolysis to the vectoral process involved in dynein motility (Jencks, 1980). As was emphasized by Eisenberg & Hill (1985) in their model for myosin, the mechanism of energy coupling is based upon the free energy of ATP binding to the enzyme under cellular conditions. Release of products is favored due to low physiological concentrations of ADP and phosphate and to their increased stability in solution, so that in the cell this step should also occur with a large free-energy change. The hydrolysis of bound ATP is required in order to convert a tight-binding ligand to a form which binds more weakly. Thus, energetically, ATP hydrolysis at the active site is relatively unimportant and occurs with only a small change in free energy.

Using the value for the rate of release of ATP from the myosin–ATP complex measured here, and the rate of binding of ATP to myosin, which was measured as 6.6×10^6 M^{-1} at 28 °C, pH 7, in 50 mM PIPES (T. J. Chilcote and K. A. Johnson, unpublished results; Johnson, 1985), an equilibrium constant of 3×10^9 M^{-1} can be calculated. Thus, the two major motility enzymes differ in that ATP binding is 100-fold tighter for myosin than for dynein. Myosin also seems to bind ADP and phosphate more tightly, as is reflected in the significantly different degrees of product inhibition measured here. In general, however, the similarities of the two enzymes extend to the thermodynamics of nucleotide binding in that the major decrease in free energy occurs with substrate binding, not ATP hydrolysis. This energy of binding is used by the enzymes to drive the dissociation of the cross bridges in the motility cycle.

Acknowledgments

We thank Karen Arndt for performing the initial phosphate–water oxygen exchange experiments as part of her undergraduate honors thesis and Dave Clark for analyzing the [^{18}O]phosphate distributions by ^{31}P NMR.

Registry No. ATP, 56-65-5; ATPase, 9000-83-3; PO_4^{3-}, 14265-44-2.

References

Barclay, R., & Yount, R. G. (1972) *J. Biol. Chem. 247*, 4098–4100.

Bergmeyer, H.-U. (1963) *Methods of Enzymatic Analysis*, p 1965, Verlag Chemie, Academic Press, New York.

Cardon, J. W., & Boyer, P. D. (1978) *Eur. J. Biochem. 92*, 443–448.

Cohn, M., & Hu, A. (1978) *Proc. Natl. Acad. Sci. U.S.A. 75*, 200–203.

Eisenberg, E., & Hill, T. L. (1985) *Science (Washington, D.C.) 227*, 999–1006.

Feldhaus, P., Frohlich, T., Goody, R. S., Isakov, M., & Schirmer, R. H. (1975) *Eur. J. Biochem. 57*, 197–204.

Froelich, J. P., Sullivan, J. V., & Berger, R. L. (1976) *Anal. Biochem. 73*, 331–341.

Goody, R. S., Hofmann, W., & Mannherz, H. G. (1977) *Eur. J. Biochem. 78*, 317–324.

Hackney, D. D. (1980) *J. Biol. Chem. 255*, 5320–5328.

Hackney, D. D., Stempol, K. E., & Boyer, P. D. (1980) *Methods Enzymol. 64*, 60–83.

Jencks, W. P. (1980) *Adv. Enzymol. Relat. Areas Mol. Biol. 51*, 75–107.

Johnson, K. A. (1983) *J. Biol. Chem. 258*, 13825–13832.

Johnson, K. A. (1985) *Annu. Rev. Biophys. Biophys. Chem. 14*, 161–188.

Kuleva, N. V., Shanina, N. A., & Krasovskaya, I. E. (1983) *Biochemistry (Engl. Transl.) 48*, 1459–1464.

Lanzetta, P. A., Alvarez, L. J., Reinach, P. S., & Candia, O. A. (1979) *Anal. Biochem. 100*, 95–97.

Lienhard, G. E., & Secemski, I. I. (1973) *J. Biol. Chem. 248*, 1121–1123.

Lowry, O. H., & Passonneau, J. V. (1972) *A Flexible System of Enzymatic Assays*, Academic Press, New York.

Omoto, C. K., & Johnson, K. A. (1986) *Biochemistry* (preceding paper in this issue).

Porter, M. E., & Johnson, K. A. (1983a) *J. Biol. Chem. 258*, 6575–6581.

Porter, M. E., & Johnson, K. A. (1983b) *J. Biol. Chem. 258*, 6582–6587.

Risley, J. M., & Van Etten, R. L. (1978) *J. Labelled Compd. Radiopharm. 15*, 533–537.

Shimizu, T. (1981) *Biochemistry 20*, 4347–4354.

Shimizu, T., & Johnson, K. A. (1983a) *J. Biol. Chem. 258*, 13833–13840.

Shimizu, T., & Johnson, K. A. (1983b) *J. Biol. Chem. 258*, 13841–13846.

Sleep, J. A., & Hutton, R. L. (1978) *Biochemistry 17*, 5423–5430.

Sleep, J. A., Hackney, D. D., & Boyer, P. D. (1978) *J. Biol. Chem. 253*, 5235.

Summers, K. E., & Gibbons, I. R. (1971) *Proc. Natl. Acad. Sci. U.S.A. 68*, 3092.

Taylor, E. W. (1977) *Biochemistry 16*, 732–739.

Weeds, A. G., & Taylor, R. S. (1975) *Nature (London) 257*, 54–56.

Weeds, A. G., & Pope, B. (1976) *J. Mol. Biol. 111*, 129–157.